Methods to Enhance Electrical Conductivity of PEDOT:PSS-based Electrodes

Amrita Chakraborty, Aaron Di Filippo, Sheena Deivasigamani, Calvin Hong, Anshu Madwesh, Marius Orlowski*

Bradley Department of Electrical and Computer Engineering, Virginia Tech, Blacksburg, Virginia 24061, USA

Research Article

ABSTRACT

This paper extends our prior study on enhancing Poly (3,4-ethylenedioxythiophene) Polystyrene Sulfonate (PEDOT:PSS) electrical conductivity. We explore various methods, including acid treatments, metal nanoparticle doping (Cu and Ag), multiple PEDOT:PSS layer depositions, and mono/multiatomic layer graphene insertion. Our findings reveal that optimizing PEDOT:PSS multilayer depositions and the treatment with nitric acid surpasses the effectiveness of additional methods using metal nanoparticles and graphene. This optimized process not only enhances PEDOT:PSS electrical conductivity but also proves less error-prone, more stable, and more cost-effective than using graphene layers and metal nanoparticles. Optimization factors include spinning speed, etchant concentration, and etching time. Compared to a single-layer PEDOT:PSS of the same thickness, the optimized multilayer PEDOT:PSS treated with nitric acid shows a reduction in sheet resistance from 1 MΩ/sq to 7 Ω/sq. Additionally, we account for film aging to mitigate ambient-induced reliability effects.

Keywords: Polystyrene Sulfonate; Metal Nanoparticle

INTRODUCTION

In our previous study, we introduced a novel method for producing conductive organic electrodes using doped PEDOT-PSS polymer films. Our findings revealed the extraordinary potential of these electrodes, showcasing their ability to be patterned and robust adhesion to diverse substrates, ranging from oxidized silicon wafers to flexible materials like Mylar.

Journal of Material Sciences

Effective substrate adhesion was achieved through a simple oxygen plasma cleaning step. To pattern the PEDOT:PSS films, we introduced a sacrificial silver metal layer to prevent chemical deterioration of PEDOT:PSS when exposed to standard photolithography process solvents. Key findings from reference include a remarkable increase in electrical conductivity (by over two orders of magnitude) through multiple PEDOT:PSS depositions, without a significant increase in film thickness [1]. An exponential relationship emerged as we observed a fundamental dependency between sheet resistance and the number of PEDOT:PSS coatings, deepening our understanding of the roles of PEDOT (the conductive component) and PSS (the non-conductive component) within the deposited PEDOT:PSS material. In the absence of other enhancement techniques, additional PEDOT:PSS coatings beyond six layers yield diminishing returns in terms of lowering the sheet resistance. However, in conjunction with acid treatments investigated in this study, the point at which only negligible improvements are obtained increases to about 9-10 coatings to compensate for the material loss due to acid treatment.

Furthermore, in our previous work, we explored the introduction of Cu Nano Particles (Cu NPs) as a doping agent, applied topically to soft-baked PEDOT:PSS films, revealing another remarkable leap in electrical conductivity again, by two orders of magnitude. However, we encountered a notable counteractive effect: the two methods of conductivity enhancement, multiple PEDOT:PSS coatings, and Cu NP doping, did not simply add up as anticipated. In other words, combining these two methods did not yield cumulative improvements.

In earlier studies, the addition of metal nanoparticles to PEDOT:PSS has attracted a lot of interest. For example, X. Zhang et al., Successfully produced PEDOT:PSS thin films doped with silver nanoparticles using inkjet printing, resulting in remarkable electrical and optical capabilities. In a similar vein [2]. Reported that doping PEDOT:PSS with silver nanoparticles increased its conductivity. R.-C [3]. Demonstrated the effectiveness of gold nanoparticle-PEDOT:PSS nanocomposites as catalysts in alkaline direct ethanol fuel cells by introducing a simplified synthesis procedure for their creation[4]. Used silver particles produced by gamma radiation to improve PEDOT:PSS conductivity, especially when it came to organic solar cells [5]. Finally, strong evidence of notable improvements in polymer conductivity when Cu NPs were used as dopants was presented [6].

In this article, we continue our exploration of ways to enhance electrical conductivity of PEDOT:PSS layers and present novel techniques that extend and complement our previous work. Specifically, we examine treatments with nitric, phosphoric, and sulfuric acids, along with the effects of introducing noble metal nanoparticles and mono- and multi-layer graphene. In case of the acid treatment methods, nitric acid treatment emerges as a standout performer among the acid treatments, with its optimization as a focal point in our investigation. We have also examined how environmental conditions affect the organic electrodes treated by acids by storing them in standard laboratory conditions and vacuum chambers for up to two weeks.

The use of acids to enhance the conductivity of PEDOT:PSS films has been explored in previous studies. Phosphoric acid treatment of individual PEDOT:PSS films was applied for 0.5 and 10 minutes in a study by [7]. Their research showed that the PSS component could be efficiently eliminated by using phosphoric acid, which improved electron extraction and improved solar cell device performance. They came to the conclusion that too much PSS impaired the gadgets' ability to gather electrons. Our findings corroborate this judgment and imply that treating solar cells with nitric acid may improve their efficiency even further. F. Zhang's group also demonstrated the production of semitransparent polymer solar cells (PCS) with a power conversion efficiency of 9.40% and a visual transmittance of 24.6% in their research [8]. Additionally, they tuned PCS to have a 15.6% power conversion rate, showing poor transmittance in the near-infrared spectrum and high transmittance in the visible light range [9]. Additionally, showed

how to use a post-spin-rinsing technique to produce highly conductive PEDOT:PSS transparent electrodes for polymer solar cells [10]. In our earlier research, we investigated the application of Cu NPs topically and discovered that bulk doping of Cu was ineffective due to oxidation in aqueous solutions. In this new study, we employ noble metal nanoparticles, specifically silver, which facilitate beneficial bulk doping of the PEDOT:PSS layers.

Here, we also explore the insertion of graphene monolayers and trilayers to enhance the conductivity of PEDOT:PSS. Graphene has been previously employed in various forms to enhance the electrical conductivity of PEDOT:PSS films, resulting in significant improvements. In reference, PEDOT:PSS films were doped with graphene composites for applications in energy harvesting systems [11]. The graphene composites were dispersed in a solution of PSS, and their content was varied to obtain the highest electrical conductivity. A 41% improvement in conductivity was achieved over unhoped PEDOT:PSS. Overall, the conductivity improvement led to a 93% higher power factor than the device based on pristine PEDOT:PSS. A similar doping technique of PEDOT:PSS with graphene composites, combined with treatment of concentrated H_2SO_4, has been employed by M. Zhang to enhance the electrocatalytic activity for the oxygen reduction reaction at the cathodes of fuel cells and metal-air batteries [12]. The resultant PEDOT:PSS/graphene composites exhibit synergistically enhanced electrocatalytic activity, better tolerance to the methanol crossover effect and CO poisoning, and improved durability over that of a Pt/C electrode.

Doping of PEDOT:PSS with reduced graphene oxide-carbon nanotubes has been used by P.C. To enhance the conductivity of the polymer films for transparent electrode applications [13]. A maximum conductivity of 3804 S/cm has been observed, which is comparable to that of indium oxide (4000 S/cm). In reference, PEDOT:PSS films were doped with graphene and graphene quantum dots, showing that both graphene and graphene quantum dots improve the conductivity of PEDOT:PSS films with only a small decrease in transparency (13-14%) [14].

Stable and highly conductive polymer films have been obtained by doping PEDOT:PSS with graphene nanocomposites for biosensor applications [15]. Graphene Nano Platelet (GNP) composites were deposited on Fluoride Tin Oxide (FTO) *via* the electrospray technique from a mixture solution of PEDOT:PSS and GNPs, which was subsequently treated with H_2SO_4 acid. Such an enhanced FTO electrode showed very high catalytic activity for the detection of dopamine, easily differentiating the electrochemical oxidation signals of ascorbic and uric acids.

Demonstrated a flexible sensor with graphene oxide/PEDOT:PSS composites for voltammetric determination of selective low levels of dopamine [16]. The sensor showed a dopamine detection limit of 0.008 µM and a sensitivity of 69.3 µA/µMcm².

Achieved high conductivity polymer films by doping PEDOT:PSS with Graphene Quantum Dots (GQD) [17]. An electric conductivity of 7172 S/m was observed, which is 31% higher than that of pristine PEDOT:PSS. The thermal conductivity experienced an even higher improvement of 113% than that of pristine PEDOT:PSS. PEDOT:PSS/GQDs were prepared *via* a simple casting method. The strong π-π bonding between GQDs and PSS chains led to decoupling and phase separation of PEDOT:PSS and PSS chains, resulting in higher electrical and thermal conductivities.

Combined PEDOT:PSS with exfoliated graphene to provide an alternative to indium tin oxide in optoelectronic devices [18]. The graphene flakes were synthesized *via* the graphite exfoliation method. A good compromise, as a function of the graphene content, was achieved, with the conductivity and optical transparency as high as 4.2×10^3 S/cm and 94%, respectively.

In reference, an electrochromic device was successfully fabricated using PEDOT:PSS and graphene as active, flexible conductive electrode films [19]. In their work, S.K Nemani apply the wrinkling instability of graphene to impart hydrophobic properties to the electrode [9]. A wide range of color contrast, flexibility, and anti-wetting nature of the

device has been achieved O. Faruk et al., A comprehensive review of various doping techniques of PEDOT:PSS with graphene and its derivatives, such as graphene oxide, reduced graphene oxide, and graphene quantum dots, has been given by G. J [20]. Recent advances in the integration of PEDOT:PSS with graphene and its derivatives for applications in energy storage devices, such as super capacitors, have been described in much detail [21].

Our objective of the continuation of the precursor work is also to assess the compatibility of various conductivity enhancement methods and explore potential synergies [1]. The dispersion of silver nanoparticles, whether applied topically or introduced as bulk doping, reveals promising effects though interestingly, their conjunction with acid treatment does not yield further major enhancements.

The main objective of this paper is to develop organic electrodes embedded with copper or silver particles for nonvolatile ReRAM memory arrays on flexible substrates. It is well-established that ReRAM arrays function optimally when constructed with Cu and Ag particles as building components for the filaments connecting the two electrodes of a ReRAM cell. Given our focus on organic ReRAM memory, other properties of these films, such as transparency, are not pertinent to our application. Consequently, no analysis of the transmittance of the multi-layer PEDOT:PSS has been conducted. However, favorable transparency characteristics could prove advantageous if, in the future, our organic memory arrays were to be integrated with solar cells for power supply purposes.

Moving on to the results section, we first present the individual effects of Nitric, Phosphoric, and Sulfuric Acids (HNO_3, H_3PO_4, and H_2SO_4) as well as the effects of topical and bulk doping of PEDOT:PSS with silver nanoparticles. In this initial part, we concentrate on the outcomes of each technique in isolation. Subsequently, in the latter part of the Results section, we delve into the synergistic effects that emerge when these techniques are combined with the multi-layer PEDOT:PSS deposition process. Finally, we summarize the most significant findings of the paper in the concluding remarks section.

MATERIALS AND METHODS

Electrode fabrication

The fabrication of organic electrodes commenced with the utilization of a commercial dispersion of PEDOT:PSS in water. This dispersion was employed to deposit organic films onto cleaned substrates, which included oxidized Si wafers and flexible mylar substrates. We utilized the spin-coating technique for film deposition, with the spin speed ranging from 500 rpm to 3000 rpm. This choice of spin speed was especially crucial for multilayer PEDOT:PSS stacks, where each layer's speed, including speed ramps, had to be carefully selected to achieve the desired film thickness and the lowest achievable sheet resistance. The subsequent application of oxygen plasma cleaning significantly enhanced the uniformity of these films.

To measure the film thickness accurately, the PEDOT:PSS films have been patterned to form a step. In the previous paper, we showcased the patterning of highly conductive polymer films using photolithography [1]. This process employed a novel flow that relied on sacrificial metal layers. We successfully addressed adhesion issues and demonstrated that, with carefully calibrated process recipes, highly conductive PEDOT:PSS films can be patterned on both Si-wafer and flexible substrates like mylar. This advancement opens avenues for the deployment of flexible electronics. Dektak profilometer and Atomic Force Microscopy (AFM) were utilized to determine the thickness of PEDOT:PSS films, yielding thickness differentials results of ± 1 nm. An optical microscopy image of a step of a patterned PEDT:PSS film is given in Figure 1(a) along with the AFM image of the measurement of the film's thickness by AFM shown in Figure 1(b). The thickness of the PEDOT:PSS layer depends on the spinning speed and on the numbers of PEDOT:PSS coatings, as shown in Table 1. A 3 × PEDOT:PSS, for example, deposited at speeds of 1500,

2000 rpm and 3000 rpm, for the 1st, 2nd, and 3rd deposition results in a total film thickness of 72 nm, which is at variance with the purely additive sum of 65+56+29=150 nm and merely 7 nm thicker than a 1 × PEDOT:PSS (65 nm) spun at 1500 rpm.

Regardless of whether the acid treatment targets a single or multiple layers of PEDOT:PSS, its core action involves the removal of PSS from the upper layer. The residue comprises a layer primarily composed of PEDOT, occasionally housing residual PSS inclusions, as illustrated in Figure 2.

Table 1: The effective film thickness (nm) at different spinning speeds for 1 × PEDOT:PSS, 3 × PEDOT:PSS, and 6 × PEDOT:PSS stacks.

PEDOT:PSS	1 ×	1 ×	1 ×	3 ×	3 ×	6 ×
Speed in rpm	1500	2000	3000	1500, 3000, 1500	1500, 2000, 3000	1500, 2000, 4×3000
Thickness (nm)	65	56	29	85	72	120

Figure 1. a) optical microscopy image of the patterned edge of a 6 × PEDOT:PSS stack, b) AFM image of the step in the 6 × PEDOT:PSS stack.

a) Patterned edge of 6× PEDOT:PSS

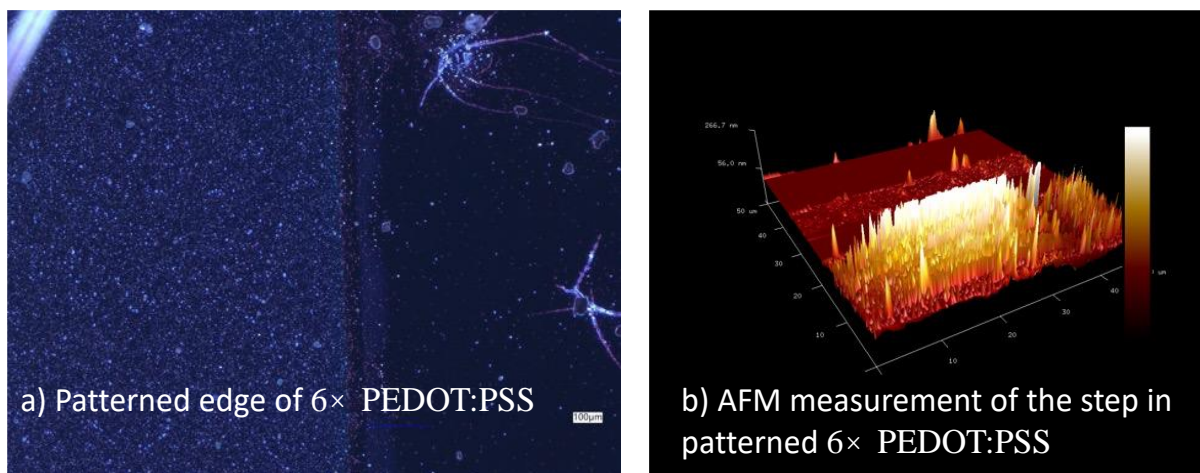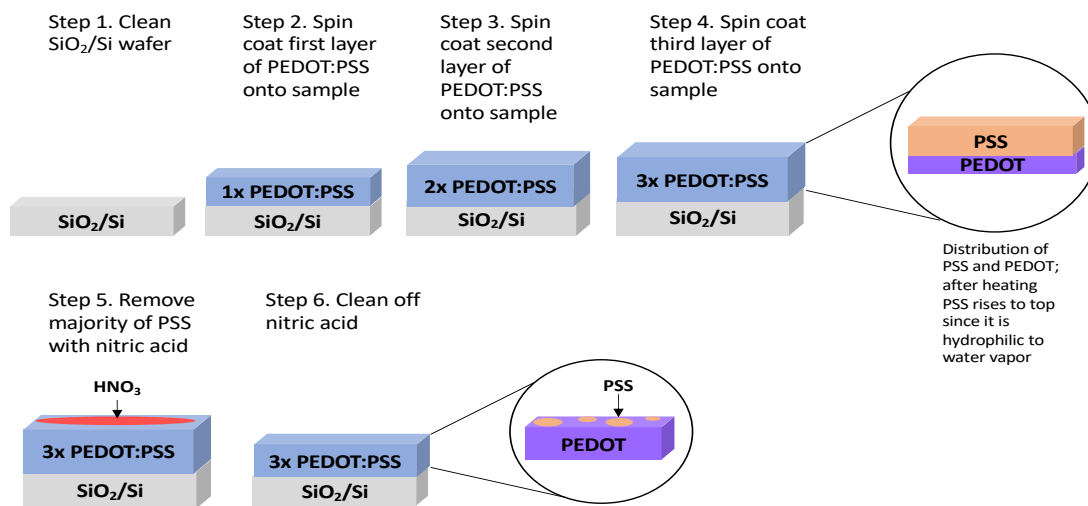b) AFM measurement of the step in patterned 6× PEDOT:PSS

Figure 2. Process steps of acid treatment of multilayer PEDOT:PSS films. The acid treatment results in removal of the top portion of PSS leaving only PSS inclusions within the PEDOT phase.

Journal of Material Sciences

We conducted experiments involving the application of silver nanoparticles (Ag NPs) to multilayer PEDOT:PSS using both the topical and bulk doping approaches. For bulk doping, 5 mg of Ag NPs was combined with 10 ml of PEDOT:PSS solution to make a 0.5 mg/ml concentration solution. The mixture was stirred for a minimum of 1 hour and subsequently sonicated for an additional hour. In contrast, for surface doping, a dispersion solution of Ag NPs in ethanol of same 0.5 mg/ml concentration was prepared, followed by the same stirring and sonication procedure employed in the bulk doping method. The dispersion of Ag nanoparticles in ethanol was subsequently spin-coated onto the surface of the PEDOT:PSS layer at 1500 rpm.

The choice of silver nanoparticle concentration at 0.5 mg/ml was informed by our earlier research involving copper nanoparticles [1]. In a prior study, we explored different concentrations of Cu NPs, specifically 0.2 mg/ml and 0.5 mg/ml, and determined that the latter (0.5 mg/ml) yielded the most favorable outcomes. To maintain consistency, we opted for the same concentration (0.5 mg/ml) when working with silver nanoparticles.

Regarding the silver nanoparticles, we had access to two powders from sky springs nanomaterials, Inc., one with nanoparticles sizes ranging from 20-30 nm and another one with nanoparticles ranging from 50-60 nm, with the larger sizes providing higher conductivity of the PEDOT:PSS (see next section).

In this paper, the ultimate enhancement method under consideration entails the insertion of mono- and trilayer graphene between the oxidized Si wafer and PEDOT:PSS films [22]. Our transfer process for the graphene monolayer consisted of several steps.

- Cutting Poly Ethylene Terephthalate (PET) and the graphene-on-copper sheet into 1 cm x 1 cm squares and taping the graphene-on-copper sheet onto the PET.
- Spin-coating the poly methyl methacrylate PMMA solution onto the graphene at 500 rpm for 5 seconds, followed by 2500 rpm for 45 seconds. The PMMA solution comprised 10 mL of PMMA solution mixed with 10 mL of anisole solvent, resulting in a final concentration of 4.5% PMMA. Approximately 4 to 5 drops of this PMMA solution were dispensed onto the graphene and spin-coated. An annealing step followed, with options including 50°C for 2 minutes.
- Subsequently, PET was removed, and the sample was exposed to oxygen plasma at 30 W of power, with a gas flow rate of 10 SCCM of oxygen gas, for 1 minute.
- The copper foil was then etched away by floating it in a copper etchant ($FeCl_3$) for approximately 10 minutes until most of the copper was etched away.
- The film was transferred into DI water using a glass slide, left in the DI water for about 10 minutes, and this process was repeated two more times with fresh DI water each time.
- After the third DI bath, the graphene film was lifted onto the oxidized Si wafer sample, effecting the transfer of graphene onto the wafer.
- The sample was then air-dried for 4 hours and placed in a vacuum chamber for 12-24 hours.
- The PMMA was then removed, by initially baking the wafer at 85°C for 5 minutes, followed by a bake at 140°C for 15 minutes and then subsequently immersing the sample in warm acetone at 55°C for 1 hour.
- Finally, the sample was cleaned with Iso Propyl Alcohol cleaning solvent (IPA) for 30 minutes and dried to obtain graphene on oxidized Si wafer.

This comprehensive process ensured the successful transfer of the graphene monolayer onto the wafer. Figure 3 shows the image a monolayer graphene transferred onto an oxidized Si substrate. The graphene trilayer is provided

as a separate sample on 1 cm × 1 cm pieces of oxidized Si wafers by the company, Graphenea [22]. It consists of three graphene monolayers stacked directly upon each other.

Figure 3. Graphene monolayer transferred onto SiO$_2$/Si following the procedure outlined in the text.

The sheet resistance, denoted as R$_{sq}$, or the conductivity, symbolized as σ, of the PEDOT:PSS layers has been determined utilizing the four-probe measurement method [23]. The electrical properties, conductivity, and sheet resistance are related and can be expressed through eq. (1):

$$\sigma = \frac{1}{R_{sq} \times t}$$

For instance, let's take a pristine PEDOT: PSS film deposited at 2000 rpm, resulting in a film thickness (t) of 56 nm and possessing a sheet resistance of R$_{sq}$ equal to 1 MΩ/sq. According to eq. (1), this sheet resistance value corresponds to a conductivity (σ) value of 0.18 S/cm.

RESULTS AND DISCUSSION

We begin our investigation by examining the impact of acid treatment on a single-layer PEDOT: PSS, specifically utilizing phosphoric, sulfuric, and nitric acid. Table 2 presents the sheet resistance values obtained for these three acid treatments at a concentration of 100% for 2 seconds. As seen from Table 2, nitric and sulfuric acid outperform phosphoric acid by a factor of at least five, with nitric acid showing a slight advantage over phosphoric acid. The observed reductions in sheet resistance hold consistent across different acid concentrations and treatment durations, even with the application of a 60% acid concentration for 1 minute. Given that nitric acid consistently delivers the best results, our subsequent focus will center on the nitric acid process. When conducting experiments with nitric acid at a 100% concentration, we explored different treatment durations: 1, 2, 3, 30, 40, and 60 seconds. Our findings revealed that varying the treatment time had only a minor effect on sheet resistance, with the 2-second treatment showing a slight advantage.

Table 2: Comparison of sheet resistance of a single PEDOT: PSS layer for acids, HNO_3, H_3PO_4, and H_2SO_4.

Conductivity Enhancement Technique	Sheet Resistance (Ω/sq)
Nitric Acid (HNO_3) for 2 sec, 100% Concentration, 1 × PEDOT:PSS	172 k
Phosphoric Acid (H_3PO_4) for 2 sec, 100% Concentration, 1 × PEDOT:PSS	1.2 k
Sulfuric Acid (H_2SO_4) for 2 sec, 100% Concentration, 1 × PEDOT:PSS	220 k

Our investigation then turns to the influence of nitric acid concentration on its ability to reduce sheet resistance. Given the well-known principle that more concentrated acid solutions tend to be more effective, we sought to ensure a fair comparison by extending the treatment time to 60 seconds for all acid concentrations. The outcomes of this study are presented in Table 3. Not surprisingly, the 1 × PEDOT:PSS samples, showed that a 100% nitric acid concentration resulted in the lowest sheet resistance, measuring 130 ohms per square, while the lowest concentration of 20% led to the highest sheet resistance, measuring 1823 ohms per square. Interestingly, acid concentrations of 40%, 60%, and 80% produced comparable results in terms of sheet resistance, between 170 and 200 Ω/sq.

Table 3. Sheet resistance as a function of HNO_3 acid concentration applied for 1 min.

Conductivity Enhancement Technique	Sheet Resistance (Ω/sq)
1× PEDOT:PSS + 100% HNO_3 for 1 min	130
1× PEDOT:PSS + 80% HNO_3 for 1 min	171
1× PEDOT:PSS + 60% HNO_3 for 1 min	181
1× PEDOT:PSS + 40% HNO_3 for 1 min	201
1× PEDOT:PSS + 20% HNO_3 for 1 min	1823

In Figure 4 and Table 4, we contrast the sheet resistance of PEDOT: PSS stacks subjected to 60% nitric acid treatment with those without acid treatment, considering the number of layers.

Nitric acid treatment significantly reduces sheet resistance by approximately two orders of magnitude for all numbers of PEDOT: PSS coatings. Notably, the best result achieved is 7.7 Ω/sq for 9 × PEDOT: PSS layers treated with 60% nitric acid. It is important to highlight that this study builds upon our earlier research, pushing the analysis beyond the previous maximum of 6 PEDOT: PSS layers to now include 9 layers [1]. The incorporation of these additional 3 layers leads to a threefold reduction in sheet resistance. Nevertheless, subsequent increases (more than 9 coatings) in the number of layers yield only marginal enhancements.

Journal of Material Sciences

Figure 4. The upper figure depicts the sheet resistance on a linear scale for the multi-layer PEDOT:PSS system untreated by HNO_3 acid. The lower figure provides a comparison of sheet resistance on a logarithmic scale between the multilayer PEDOT:PSS stack treated with HNO_3 and the untreated stack.
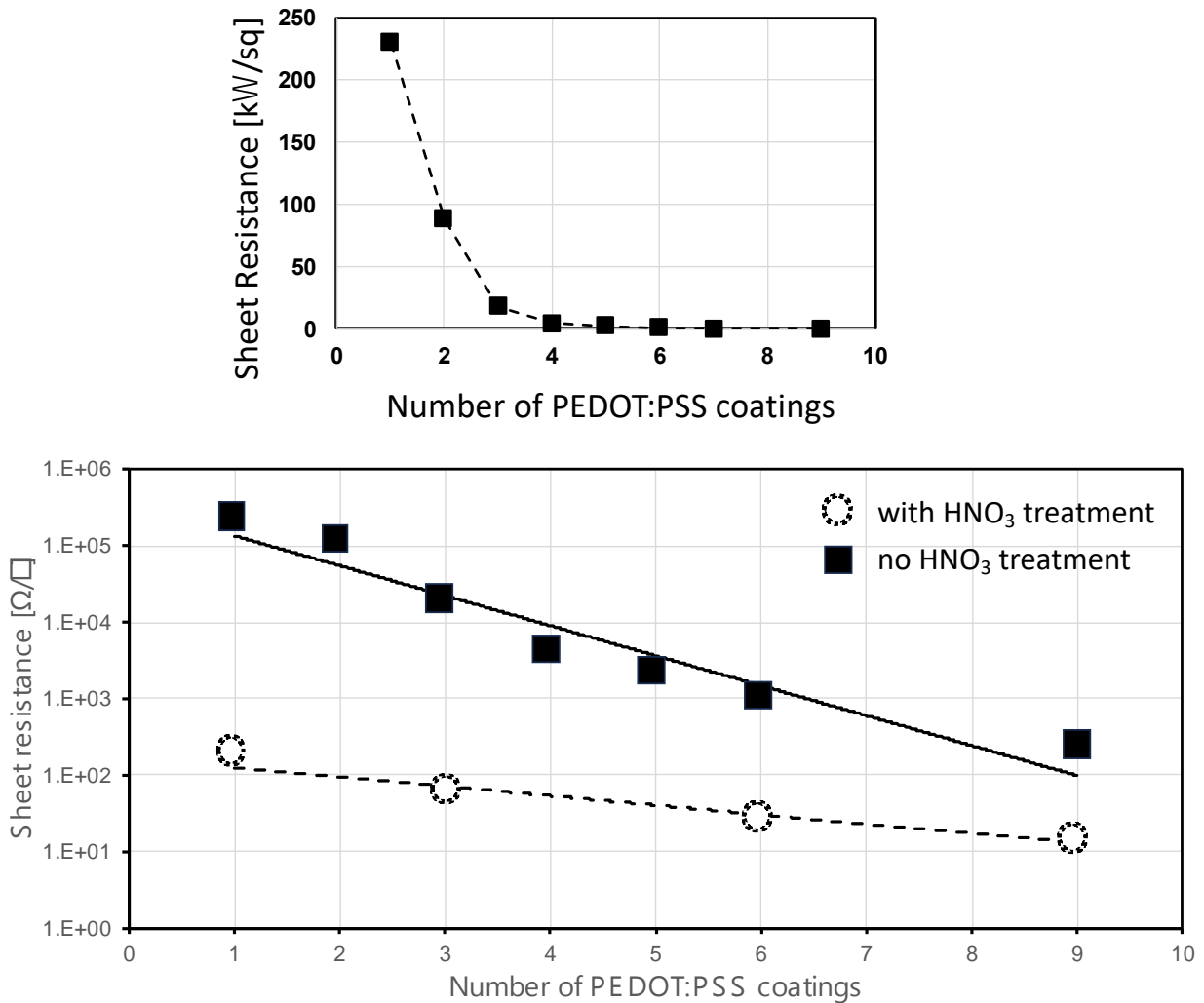
Table 4. Sheet resistance of multilayer PEDOT:PSS layer stacks as a function of the number of layers with and without nitric acid treatment.

Conductivity Enhancement Technique	Sheet Resistance w/ 60% HNO_3 for 1 min (Ω/sq)	Sheet Resistance w/o HNO_3 (Ω/sq)
1 × PEDOT:PSS	181	230 k
3 × PEDOT:PSS	51	18 k
6 × PEDOT:PSS	22	906
9 × PEDOT:PSS	7.7	37.73

Journal of Material Sciences

The extension from 6 to 9 layers, especially in the case of acid treatment, suggests that the extra 3 layers serve to compensate for the material loss incurred during the etch treatment. As described in more detail elsewhere, during the spin deposition of PEDOT:PSS, a vertical phase separation phenomenon occurs, segregating the PEDOT and PSS components [1]. The resulting wet film accumulates conductive PEDOT strips at its base and a PSS-rich solution at the upper segment. The transition between PEDOT and PSS phases is, of course, not abrupt but gradual, with the highest concentration of PSS at the top and the lowest at the bottom, exhibiting an opposite behavior for PEDOT. With the application of each successive PEDOT:PSS layer, the PEDOT component of the subsequent coating permeates through the soluble PSS of the preceding layer, leading to the thickening and consolidation of the combined PEDOT phase at the base. Following this, when acid treatment is applied, the upper portion of the layer containing the non-conductive PSS phase is eliminated. It is crucial to highlight that during the acid treatment process, a considerable portion of PSS inclusions within the PEDOT phase is expected to be removed, thereby improving the conductivity of the resultant layer.

Our attention now shifts to the potential of silver nanoparticles (Ag NP) to enhance the electrical conductivity of PEDOT:PSS. Given silver's inert nature, we introduced it using two methods: bulk doping, where Ag NP dispersion was mixed with PEDOT:PSS solution, and topical application after a soft bake of the PEDOT:PSS. Two sizes of Ag NP, ranging from 20-30 nm and 50-60 nm, were employed. Our experiments reveal that larger Ag nanoparticles consistently yield higher conductivity values. Table 5 compares bulk and topical applications of Ag NP for 1 × PEDOT:PSS and 3 × PEDOT:PSS.

Topical Ag NP application results in significantly lower sheet resistance compared to the bulk method, demonstrating a three-order-of-magnitude improvement. Hence, this method might be preferable in applications such as ReRAM cells where the presence of Cu or Ag is highly desirable [24-27].

This suggests that even in the case of noble metal nanoparticles, bulk doping with nanoparticles is ineffective due to potential issues such as inadequate accommodation of Ag NP within PEDOT:PSS and possible coating of Ag NP by PSS. To the best of our knowledge, there are no existing reports on the topical application of metal nanoparticles in PEDOT:PSS.

Table 5. Sheet resistance of 1 × PEDOT:PSS and 3 × PEDOT:PSS with bulk and topical doping with Ag nanoparticles.

Conductivity Enhancement Technique	Sheet Resistance (Ω/sq)
1 × PEDOT:PSS + 100% HNO_3 for 1 min	130
1 × PEDOT:PSS + 80% HNO_3 for 1 min	171
1 × PEDOT:PSS + 60% HNO_3 for 1 min	181
1 × PEDOT:PSS + 40% HNO_3 for 1 min	201
1 × PEDOT:PSS + 20% HNO_3 for 1 min	1823

Given the inefficacy of bulk doping with Ag NP, we proceeded to compare the results with topical application of copper nanoparticles (Cu NP), a method utilized in our previous study. For 3 × PEDOT:PSS layers, both Ag and Cu NP resulted in comparable sheet resistance values of 121-260 Ω/sq and 173-256 Ω/sq, respectively. Additionally, both types of nanoparticles produced similar effects on sheet resistance for 3 × PEDOT:PSS layers treated with 60% HNO_3 acid. Therefore, it can be concluded that Cu nanoparticle doping offers an economically advantageous alternative to silver

particle doping. As documented in the literature, both Ag and Au nanoparticles, when employed in bulk doping, result in comparable levels of conductivity enhancement in PEDOT:PSS films [3,4]. Consequently, our earlier conclusion regarding the limited effectiveness of bulk doping compared to topical doping is likely applicable to Au NPs as well. In Figure 5, optical microscopy and AFM images showcase the 1 × PEDOT:PSS 1500 rpm and 3×PEDOT:PSS 1500 rpm doped with Cu NPs. The Cu NPs (size ranging from 20 nm to 30 nm) are identifiable by their orange glint. According to the AFM measurements the root mean square surface roughness of 1×PEDOT:PSS was 2.01 nm and the surface roughness increased for multilayer PEDOT:PSS to 2,42, 2,37, and 2.29 nm, for 3 × PEDOT:PSS, 6 × PEDOT:PSS, and 9 × PEDOT:PSS, respectively.

Now, we delve into the finer details of nitric acid treatment. Various concentrations ranging from 0% to 100% and different treatment times were tested. The effectiveness of sheet resistance reduction was found to be relatively independent of treatment time within the 1-second to 1-minute range. To ensure consistent treatment duration and minimize possible human errors, a baseline procedure of 1-minute duration was adopted, with similar results observed for 30-second and 40-second durations.

Figure 5. Optical microscopy and AFM images showcase the 1 × PEDOT:PSS 1500 rpm and 3 × PEDOT:PSS 1500 rpm doped with Cu NPs. The Cu NPs (size ranging from 20 nm to 30 nm) are identifiable by their orange glint.
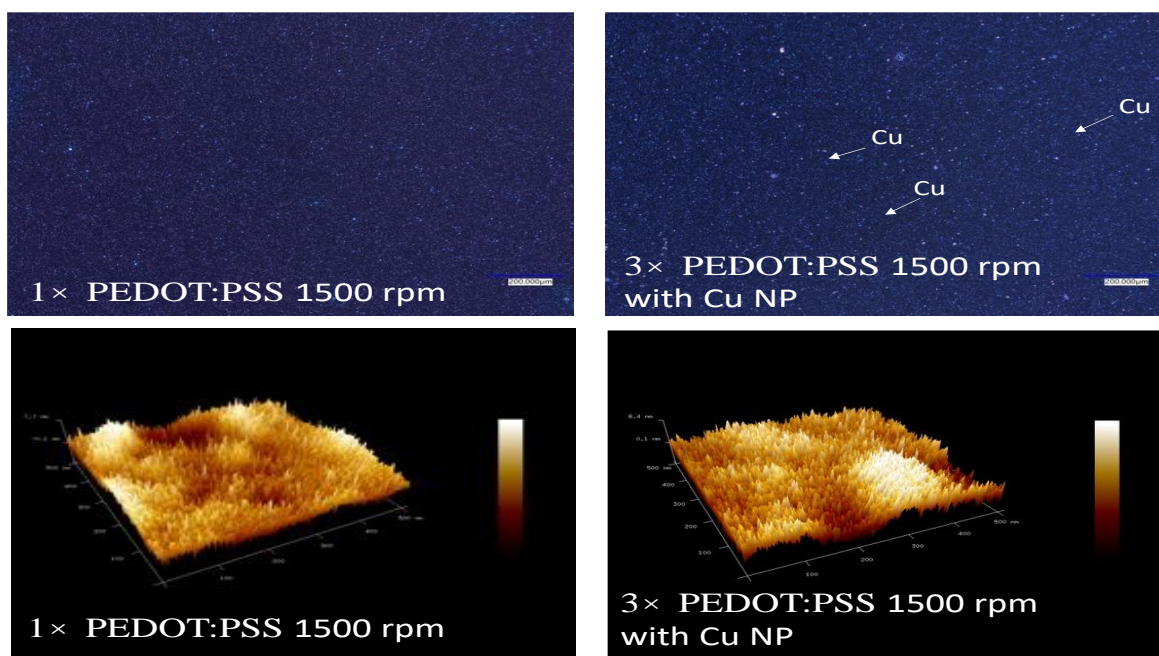
Additionally, the stability of nitric acid treatment over time was assessed. Samples were allowed to sit for several days, and sheet resistance was monitored periodically. The outcomes of the experiments are visually represented in Figure 6. Over time, it becomes apparent that the sheet resistance experiences deterioration across all acid concentrations, eventually reaching a point of saturation and maintaining relatively constant values after approximately six days.

Figure 7 regraphs the data from Figure 6, representing sheet resistance degradation (D%) as defined by the below equation.

$$D\% = \frac{\text{sheet resistance at day measured} - \text{sheet resistance just after being manufactured}}{\text{sheet resistance just after being manufactured}}$$

It is notable from Figure 7 that the sheet resistance exhibits its most stable performance at a 60% concentration of nitric acid. Consequently, for the experiments discussed earlier, we adopted the 60% nitric acid concentration as our baseline method. The intriguing aspect of sheet resistance degradation following acid treatment prompted an investigation into its potential causes. One hypothesis proposed that the degradation might arise from a reaction between the PEDOT:PSS treated with acid and the ambient laboratory atmosphere. To validate this assumption, we created identical samples, placing some in the ambient laboratory atmosphere and others in a small vacuum chamber, from which the samples were removed for a brief period to measure sheet resistance.

Figure 6. Sheet resistance stability as a function of ambient exposure for 20%, 40%, 60%, 80% nitric acid concentration. Note: (★)20%, (◆)40%, (▲)60%, (■)80%, (●)100%.
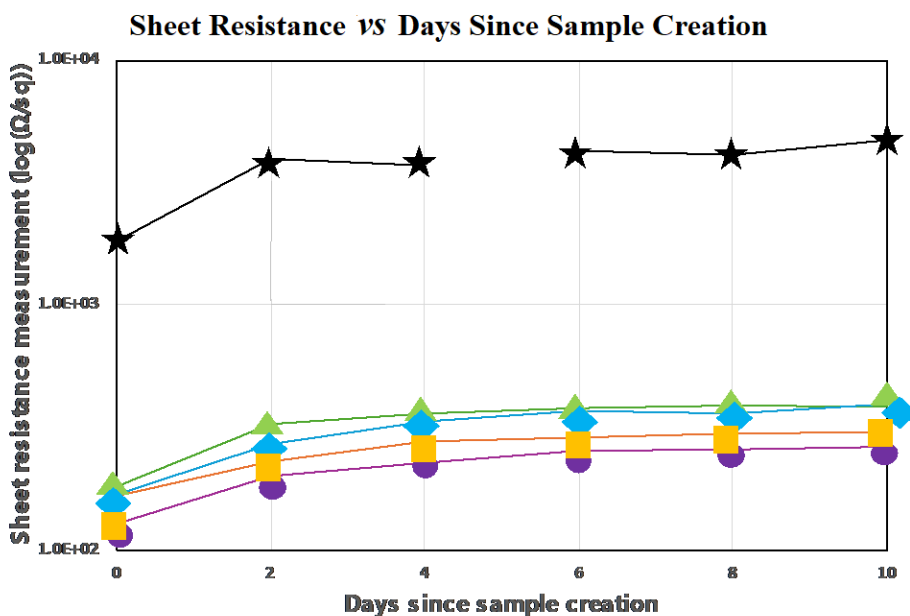

Sheet Resistance *vs* Days Since Sample Creation

Figure 7. Sheet resistance degradation as a function of ambient exposure for 20%, 40%, 60%, 80% nitric acid concentration. Note: (★)20%, (◆)40%, (▲)60%, (■)80%, (●)100%.
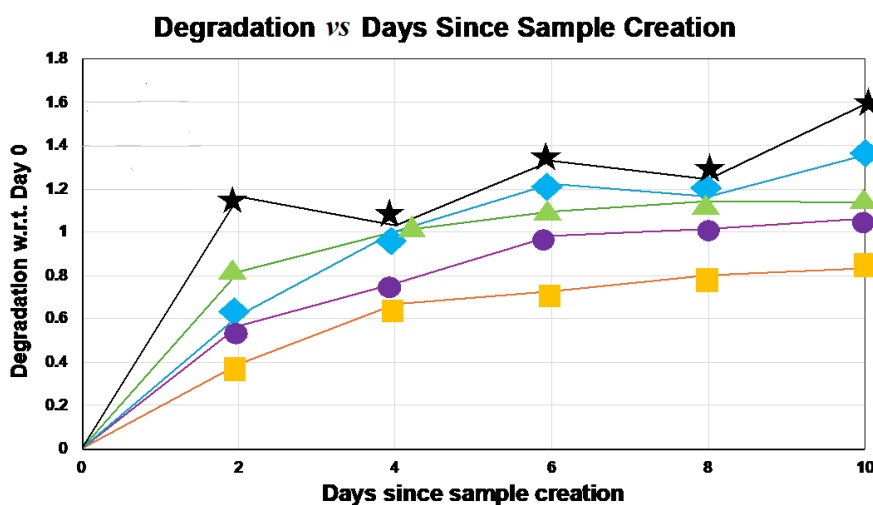

Degradation *vs* Days Since Sample Creation

Figure 8 presents the results for samples stored in both ambient laboratory conditions and the vacuum chamber. Remarkably, there was no substantial difference observed in sheet resistance between the two environments. Consequently, we conclude that the degradation is not triggered by a reaction between the samples and the ambient atmosphere but rather stems from an internal reaction within the PEDOT:PSS material itself. This observation is

fortuitous, considering the limited supply of nm-thin films for this reaction. It also elucidates why the degradation eventually reaches a saturation point over time.

Figure 8. Sheet resistance evolution as a function of time (days) for nitric acid treatment at concentration of 20%, 40%, 60%, 80%, and 100% of HNO_3. Note: (◆) 60% HNO_3+Ag NP topical in Vacuum, (■) 60% HNO_3+Ag NP topical in Lab, (▲) 60% HNO_3 in Vacuum, (⬤) 60% HNO_3 in LAB.
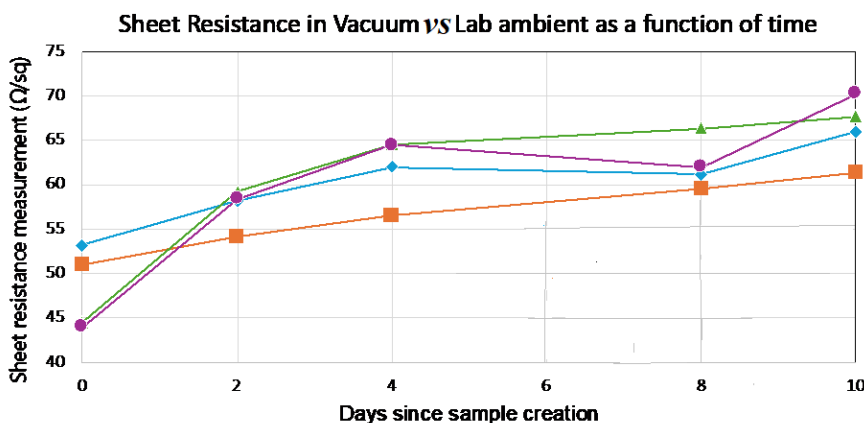
The third approach aimed at reducing PEDOT:PSS sheet resistance involved introducing graphene on an oxidized Si wafer before PEDOT:PSS layer deposition. Two types of graphene were tested: A single large graphene monolayer and trilayer graphene, as described in the previous section. The sheet resistance for the graphene monolayer was measured at 20 kΩ/sq, while the trilayer graphene exhibited significantly lower resistance at 50 Ω/sq.

It should be noted that when using trilayer graphene, adhesion issues with PEDOT:PSS were encountered. We addressed this challenge by subjecting the trilayer graphene to plasma treatment, significantly improving PEDOT:PSS adhesion to the trilayer graphene. This adhesion improvement came, however, at a cost, as the sheet resistance of the trilayer graphene deteriorated considerably. Moreover, Rsq values for PEDOT:PSS with the graphene trilayer displayed a highly non-uniform distribution of sheet resistance, ranging from 14 Ω/sq to 1 kΩ/sq depending on the location of the measurement. Notably, achieving sheet resistance values as low as 14 Ω/sq at the lower end of the range through plasma treatment of trilayer graphene presents promising avenues for future exploration.

It's worth noting that the lower end of the sheet resistance spectrum for plasma-treated trilayer graphene, with values as low as 14 Ω/sq, offers some optimism for potential future studies. Effectively addressing the non-uniformity issue remains feasible, particularly considering that handling trilayer graphene is more manageable than transferring a graphene monolayer onto a substrate. However, it is important to recognize that trilayer graphene requires a film provided on oxidized Si substrates by the supplier, which imposes constraints on autonomy in the manufacturing process, particularly on commercially avialable wafer sizes. Nevertheless, we produced a single sample of 6×PEDOT:PSS on plasma-treated trilayer graphene, resulting in a sheet resistance of 1350 Ω/sq. One favorable outcome of this result is the absence of sheet resistance no uniformity across the wafer. On the other hand, a graphene monolayer combined with 9 layers of PEDOT:PSS yielded a respectable sheet resistance of 36.4 Ω/sq. However, it still falls short of the sheet resistance achieved by 9×PEDOT:PSS treated with 60% nitric acid, which resulted in Rsq=7.7 Ω/sq.

Similar to metal nanoparticles, adding graphene—in monolayer and triple-layer versions—brings advantages of its own, but it doesn't work in concert with nitric acid treatment, just like silver nanoparticles do. The optimization of the nitric acid treatment addresses the deterioration in conductivity brought on by both ambient-induced and ambient-

independent effects, as well as film aging. A significant finding in this study is the efficacy of the straightforward approach: Combining multiple PEDOT:PSS depositions with optimized nitric acid treatment, while considering the impact of acid concentration and acid treatment time. This approach surpasses the efficacy of complex methods involving metal nanoparticles and graphene layers while providing a simpler and cost-effective means of enhancing PEDOT:PSS conductivity. Compared to a single-layer PEDOT:PSS of the same thickness, the optimized multilayer PEDOT:PSS treated with optimized nitric acid shows a reduction in sheet resistance from 1 MΩ/sq to 6.7 Ω/sq, marking a tenfold improvement over the lowest sheet resistance of 62 Ω/sq achieved with 6 PEDOT:PSS layers and topical dispersion of Cu nanoparticle doping reported in our previous work [1].

Finally, let's explore the combined effects of multiple enhancement methods. To our knowledge, the combined effects of different enhancement methods have been not yet reported Firstly, we examine the combination of nitric acid treatment and silver nanoparticle doping. For 3 × PEDOT:PSS, HNO_3 treatment alone results in a sheet resistance of 50 Ω/sq, while the addition of Ag NP as a topical application yields similar results. An outlier at 25 Ω/sq has been noted, attributed to the use of a newly shipped PEDOT:PSS (refer to the remark at the end of this section).
Hence, it can be concluded that the addition of metal nanoparticles does not yield a significant improvement over nitric acid treatment alone.

An intriguing combination of enhancement methods involves the simultaneous application of nitric acid treatment and graphene insertion. While each method independently significantly reduces sheet resistance, their combined effect seems negligible. For instance, a 9 × PEDOT:PSS layer treated with nitric acid achieves a sheet resistance of 7.7 Ω/sq, and with the addition of a graphene monolayer, the sheet resistance only slightly drops to 6.9 Ω/sq. Overall, nitric acid treatment alone proves to be the most effective approach for enhancing PEDOT:PSS conductivity, with combinations offering no additional benefits. Furthermore, the nitric acid method is the least expensive and least complex when compared to metal nanoparticle doping and graphene insertion.

As a note on the margin, we would like to discuss an observation mentioned earlier in the text. A recent shipment of PEDOT:PSS from Sigma-Aldrich consistently displayed a lower sheet resistance, approximately 2-3 times lower than the initial batch received approximately a year ago. While the new material does show a slight improvement in conductivity, the observed trends and dependencies remain consistent with those of the older material. Sigma-Aldrich has not shared any details regarding the process changes that led to this conductivity improvement [28].

CONCLUSION

We have explored various methods to enhance the electrical conductivity of PEDOT:PSS films, including acid treatments, metal nanoparticle doping (Cu and Ag), multiple PEDOT:PSS layer depositions, and the insertion of mono/multiatomic layer graphene. Our investigations have revealed that while each of these methods individually leads to a substantial increase in electrical conductivity, their combined application does not yield significant improvements.

In the realm of metal nanoparticle doping, we have observed that the topical doping method outperforms bulk doping. Notably, in the case of Cu nanoparticles, which are unsuitable for bulk doping, we found them to be as effective as noble metal nanoparticles, offering a more cost-effective alternative. Furthermore, our optimization efforts led to a nitric acid treatment process that surpasses the effectiveness of additional methods involving metal nanoparticles and graphene. This optimized treatment involves nine layers of PEDOT:PSS and can reduce the sheet resistance from 1 MΩ/sq to 7 Ω/sq, an improvement of more than 105. However, it's worth noting that the electrical conductivity of

PEDOT:PSS layers treated with acid degrades over time, albeit at a modest rate, resulting in a self-limiting reaction and stabilizing after a few days at a consistent level.

Regarding graphene's role in enhancing conductivity, we discovered that trilayer graphene, despite being a more cost-effective option than monolayer graphene, faces adhesion challenges with the PEDOT:PSS layer. Adhesion issues can be mitigated through topical plasma treatment, but this intervention has implications for uniformity of the sheet resistance and degrades the electrical conductivity gains. Nevertheless, the trilayer graphene method shows promise for enhancing conductivity, pending further research and development.

We expect that the knowledge acquired through our investigation of various methods to enhance conductivity, as outlined in this paper, will aid other researchers in identifying the most appropriate strategies to improve the conductivity of organic polymers in their specific areas of study.

ACKNOWLEDGEMENTS

DATA AVAILABILITY

All data generated or analyzed during this study are included in this published article.

DISCLAIMER

In this work no plasma sample from human have been used.

REFERENCES

1. Chakraborty A, et al. Conductive organic electrodes for flexible electronic devices. Sci Rep. 2023;13:4125.
2. Xiong Z, et al. Composite inks of poly (3,4-ethylenedioxytiophene)/poly (styrenwsulfonate)/silver nanoparticles and electric/optical properties of ink-jet-printed thin films. Mater. Chem. Phys. 2013;141:416-422.
3. Patil DS, et al. Silver incorporated PEDOT: PSS for enhanced electrochemical performance, J. Ind. Eng. Chem. 2016;42:113-120.
4. Zhang RC, et al. Gold nanoparticle-polymer nanocomposites synthesized by room temperature plasma and their potential for fuel cell electrocatalytic application. Sci Rep. 2017;7:46682.
5. Ghazy OA, et al. PEDOT:PSS incorporated silver nanoparticles prepared by gamma radiation for the application in organic solar cells. J. Rad. Res. & Appl. Science. 2015;8:166-172.
6. Pham LQ, et al. Copper nanoparticles incorporated with conducting polymer: Effects of copper concentration and surfactants on the stability and conductivity. J. Colloid Interface Sci. 2012;365:103-109.
7. Wang W, et al. Patterning of PEDOT:PSS *via* nanosecong ablation and acid treatment for organic solar cells. Org. Electron. 2020;87:105954.
8. Hu Z, et al. Semitransparent ternary nonfullerene polymer solar cells exhibiting 9.40% efficiency and 24.6% average visible transmittance. Nano Energy. 2019;55:424-432.
9. Hu Z, et al. Semitransparent polymer solar cells with 12.37% efficiency and 18.6% average visible transmittance. Sci. Bull. 2020;65:131-137.
10. Zhang H, et al. Highly conductive PEDOT:PSS transparent electrode prepared by a post-spin-rinsing method for efficient ITO-free polymer solar cells. Solar Energ. Mat. & Solar Cells, 2016;144:143-149.

11. Yoo D, et al. Direct synthesis of highly conductive PEDOT:PSS/graphene composites and their applications in energy harvesting systems", Nano Res. 2014;7:717.

12. Zhang M, et al. Solution-processed pedot:pss/graphene composites as the electrocatalyst for oxygen reduction reaction. ACS Appl. Mat. & Interf. 2014;6:3587-3593.

13. Mahakul PC, et al. Preparation and characterization of PEDOT:PSS/reduced graphene oxide-carbon nanotubes hybrid composites for transparent electrode applications. J. Mater. Sci. 2017;52:5696-5707.

14. Kepic KP,et al. Preparation of PEDOT:PSS thin films doped with graphene and graphene quantum dots. Synth. Met. 2014;198:150-154.

15. Liu D, et al. Highly stable and conductive PEDOT:PSS/graphene nanocomposites for biosensor applications in aqueous medium. New J. Chem. 2017;41:15458-15465.

16. Ko SH, et al. Flexible sensor with electrophoretic polymerized graphene oxide/PEDOT:PSS composite for voltametric determination of dopamine concentration. Sci. Rep. 2021;11:21101.

17. Du FP, et al. PEDOT:PSS/graphene quantum dots with enhanced thermoelectric properties *via* strong interfacial interactions and phase separation. Sci. Rep. 2018;8:6441.

18. Badri MAS, et al. "Exfoliated graphene-alkaline lignin-PEDOT:PSS composite as a transparent conductive electrode. Nanomat. Nanotech. 2021;11:1-8.

19. Nemani SK, et al. Stretchable and hydrophobic electrochromic devices using wrinkled graphene and pedot:pss. J. Nanomat. 2018;3230293.

20. Adekoya GJ, et al. Nanocomposites of pedot:pss with graphene and its derivatives for flexible electronic applications: a review. Macromol. Mater. Eng. 2021;306:2000716.

21. O. Faruk, et al. Recent advances in PEDOT:PSS integrated graphene and MXene-based composites for electrochemical supercapacitor applications. Synthet. Metals. 2023;297: 117384.

22. Graphene on Your Substrate.

23. Olivier J, et al. Stability/instability of conductivity and work function changes of ITO thin films, UV-irradiated in air or vacuum: Measurements by the four-probe method and by Kelvin force microscopy. Synth. Metals. 2001;122:87-89.

24. Liu T, et al. Switching characteristics of antiparallel resistive switches. IEEE Electron Dev. Lett. 2012;33:429.

25. Kang Y, et al. Observation of quantized and partial quantized conductance in polymer-suspended graphene nanoplatelets. Nanoscale res. Lett. 2016;11:179.

26. Al-Mamun MS, et al. Analysis of the electrical reram device degradation induced by thermal cross-talk. advanced electronic materials. 2023;9:2201081.

27. Chakraborty , et al. Thermal reliability issues in reram memory arrays. 2023;1001963.

28. Sigma Aldrich, Copper.